The queen scallop Aequipecten opercularis: a slow domoic acid depurator?

José Luis García-Corona, Caroline Fabioux, Hélène Hégaret

The queen scallop *Aequipecten opercularis*: a slow domoic acid depurator?

José Luis García-Corona, Caroline Fabioux, Hélène Hégaret*.

Institut Universitaire Européen de la Mer, Laboratoire des Sciences de l'Environnement Marin, UMR 6539 LEMAR (UBO/CNRS/IRD/Ifremer). Rue Dumont d'Urville, Technopôle Brest-Iroise, Plouzané 29280, France.

*Corresponding author: Hélène Hegaret

Institut Universitaire Européen de la Mer, Laboratoire des Sciences de l'Environnement Marin, UMR 6539 LEMAR (UBO/CNRS/IRD/Ifremer). Rue Dumont d'Urville, Technopôle Brest-Iroise, Plouzané 29280, France.

e-mail: helene.hegaret@univ-brest.fr

Abstract

Domoic acid (DA) is a dangerous phycotoxin produced by several strains of diatoms of the genus *Pseudo-nitzschia,* and responsible for Amnesic Shellfish Poisoning (ASP) in humans. The increasingly intense ASP-outbreaks along the English Channel over the last three decades have forced persistent harvest closures of economically important and highly contaminated bivalve stocks exhibiting slow DA-depuration rates, like the king scallop *Pecten maximus*. Under this scenario, other pectinid species, such as the queen scallop *Aequipecten opercularis* have been empirically proposed as alternative resources to redress the high economic losses due to the banning of the exploitation of *P. maximus*. Nevertheless, the kinetics of DA depuration in *A. opercularis* have not been assessed so far, and its direct extraction after ASP-episodes could represent a serious threat to public health. Hence, the main objective of this work was to estimate the DA-depuration rate in the digestive gland (DG) of naturally contaminated scallops *A. opercularis* after a toxic *Pseudo-nitzschia australis* bloom subjected to experimental depuration in the laboratory for 30 days. This study also intended to go further in the knowledge about the anatomical distribution of DA in scallop tissues, and corroborate the implications of autophagy in DA-sequestration in the DG of this species as recently hypothesized. In the DG, the DA-depuration rate (0.018 day^{-1}) suggested that even with toxin burdens as low as 40 $mg \cdot kg^{-1}$ in the DG, queen scallops may remain contaminated for about 70 days, thus longer under intensely contamination scenarios. The subcellular analyses corroborated DA-sequestration mainly through late-autophagy within residual bodies in the DG, without differences in the frequencies of anti-DA labeled residual bodies across the entire depuration process. These results revealed that *A. opercularis* cannot be considered a fast DA-depurator, and represent a baseline knowledge for decision-making about harvesting natural beds of queen scallops after toxic *Pseudo-nitzschia* blooms. The findings of this work also represent a cornerstone for further research to accelerate DA-depuration in this species.

Key words: Domoic acid, Amnesic Shellfish Poisoning, *Aequipecten opercularis*, toxicokinetics, late-autophagy, residual bodies.

1. Introduction

Domoic acid (DA) is a highly potent neurotoxin synthesized by at least 28 bloom-forming species of diatoms of the genus *Pseudo-nitzschia* distributed in all the oceans around the world (Bates *et al.,* 1989; Lelong *et al.,* 2012; Bates *et al.,* 2018). This water-soluble tricarboxylic amino acid is responsible for the amnesic shellfish poisoning (ASP) syndrome in vertebrates (Lefebvre and Robertson, 2010; Trainer *et al.,* 2012; Zabaglo *et al.,* 2016). The highly detrimental effects of DA have been attributed to its neuroexcitatory action in the hypothalamus, functioning as a structural analog of glutamate, a potent neurotransmitter in the central nervous system of birds and mammals (La Barre *et al.,* 2014; Zabaglo *et al.,* 2016, Miller *et al.,* 2021). Particularly in the brain, DA exhibits an affinity ~100-fold stronger than glutamate for the N-Methyl-D-aspartate (NMDA) and the α-amino-3-hydroxy-5-methyl-4-isoxazolepropionic acid (AMPA) ionotropic glutamate receptors, as well as for kainate receptors, which results in an uncontrolled influx of calcium into the neurons, leading to degeneration and cell death, and the consequent severe damage of the hippocampus, short-term memory loss, coma, or death in fatal cases (Perl *et al.,* 1990; Ramsdell, 2007; Pulido 2008).

When outbreaks of DA-producing *Pseudo-nitzschia* are advected over shellfish beds, the organisms can ingest and accumulate high amounts of DA through suspension-feeding activity (Trainer *et al.,* 2012; Basti *et al.,* 2018). In bivalves, the digestive gland (DG) is the organ that accumulates the largest amounts of DA (up to 90% of total burdens), as in the case of the mussels *Mytilus edulis* (Bates *et al.,* 1989), the king scallop *Pecten maximus* (Blanco *et al.,* 2006), and *Placopecten magellanicus* (Gilgan *et al.,* 1996), that are capable of accumulating up to 790, 3,200 and 4,300 mg DA kg^{-1} DG, respectively. Nonetheless, profound inter-specific differences in DA depuration kinetics have been reported among groups of invertebrates (Blanco *et al.,* 2010; Dusek Jennings *et al.* 2020). In this sense, bivalves have been broadly classified as fast and slow depurators based on their capabilities to detoxify DA. The former exhibit DA depuration rates ranging from 0.1 to 2.2 day^{-1} in the visceral mass, and as fast as 0.25 to 60 day^{-1} in the DG, being capable of depurate ≥ 90% of total DA burdens within days or a few hours. This group includes several species of mussels (Novaczek *et al.,* 1992; Silvert & Subba, 1992; Wohlgeschaffen *et al.,* 1992; Mafra

et al., 2010; Blanco *et al.*, 2002b), oysters (Mafra *et al.*, 2010), clams (Blanco *et al.*, 2010; Álvarez *et al.*, 2015; Dusek Jennings *et al.* 2020) and some scallops (Wohlgeschaffen *et al.*, 1992; Álvarez *et al.*, 2020). On the other hand, species classified as slow depurators can take a few months or even a couple of years to depurate total DA. The classic examples are some commercially important bivalves like the razor clam *Siliqua patula* (Horner *et al.*, 1993; Dusek Jennings *et al.*, 2020) and the king scallop *P. maximus* (Blanco *et al.*, 2002a, 2006; García-Corona *et al.*, 2024a), with DA depuration rates as slow as ~0.02 and ~0.001 day^{-1} in the DG, respectively. Hence, the knowledge regarding DA-depuration kinetics and the physiological processes associated with long retention of this toxin is necessary to define bivalve species as fast or slow depurators.

Despite the profound differences in DA toxicokinetics among bivalves, the metabolic reasons for these variations are still unclear. There is evidence pointing that in species such as *P. maximus* the long retention of the toxin could be due to the absence of efficient membrane transporters to carry out its excretion from the digestive cells (Mauriz and Blanco, 2010), or to the presence of some high and low-affinity glutamate receptors in specific tissues, as in the case of *S. patula* (Trainer and Bill, 2004). The recent development of an anti-DA immunohistochemical (IHC) technique (García-Corona *et al.*, 2022) allowed to visualize that part of DA derived from toxic *Pseudo-nitzschia* blooms is sequestered mainly within small autophagosome-like vesicles (~1 µm; = early autophagy) in the cytoplasm of the digestive cells of *P. maximus*, as well as in larger post-autophagic residuals bodies (5-10 µm; = late autophagy) in the DG of the scallops *P. maximus* and *Aequipecten opercularis*, as well as the slipper-snail *Crepidula fornicata*, with a potential influence of DA biotransformation profiles over these subcellular features (García-Corona *et al.*, 2024b). In the case of the slow depurator *P. maximus*, the anti-DA labeled residual bodies can remain for very long time in the DG of contaminated scallops (García-Corona *et al.*, 2024a). Hence, it has been hypothesized that late autophagy could be a subcellular mechanism closely related to the long retention of remaining DA in the DG of this species.

Over the last three decades, blooms of DA-producing *Pseudo-nitzschia* have spread and intensified throughout the North European coastal area (Amzil *et al.*, 2001; Husson *et al.*, 2016; García-Corona *et al.*, 2024a,b), leading to the extensive and prolonged banning of

economically important pectinid species such as *P. maximus* due to high accumulation and long retention of DA, and the serious threat that this represents to food security and public health (MacKenzie *et al.*, 2002; Blanco *et al.*, 2002a; Leal and Cristiano, 2024). This scenario has forced the fishing industry to look for alternative species susceptible to exploitation after ASP-episodes to compensate for the severe economic losses caused by the closures of the extraction of slow DA-depurator species.

The queen scallop *Aequipecten opercularis* is a valuable fishery resource in northern Europe, and supports high commercial pressure in the inshore waters of the English Channel (Beukers-Stewart & Beukers-Stewart, 2009), cohabiting the same DA-contaminated harvest areas as king scallops during blooms of toxic *Pseudo-nitzschia* spp. (García-Corona *et al.*, 2024b). Thus, the profession has empirically suggested the exploitation of *A. opercularis* as an option to cope with the long marketing restrictions of king scallops commonly exceeding the limit of 20 mg DA kg^{-1} of flesh in the whole or individual parts (Wekell *et al.*, 2004). Nevertheless, scientific data about the level of DA-contamination and depuration kinetics in *A. opercularis* after blooms of toxic *Pseudo-nitzschia* have not been assessed so far, hindering the consideration of this resource as an alternative for commercial activities after ASP outbreaks.

This work thus aimed to estimate for the first time the depuration rate of DA in the DG of naturally contaminated *A. opercularis* to define this species as a fast or slow DA-depurator. Furthermore, with the purpose of better understanding the implications of late autophagy in DA toxicokinetics in this species as shown in García-Corona *et al.* (2024a), we also performed the time-tracking of the subcellular localization of DA in the GD, as well as the anatomical comparison of the localization of DA in different tissues of queen scallops through depuration process in the laboratory.

2. Materials and methods

2.1. Source of scallops

Thirty DA-contaminated juvenile queen scallops *A. opercularis* (3.1 cm ± 0.05 cm; 4.9 g ± 0.2 g) were dredged from a natural bed at Roscanvel (48° 18’ 3.408 " N, 4° 32’ 23.108 " O) in the Bay of Brest, France, on early April 2021, during a bloom of *Pseudo-nitzchia australis* (1×10^5 cells L^{-1} according to the REPHY, REseau d’observation et de surveillance

du PHYtoplancton et de l'hydrologie dans les eaux littorales, https://bulletinrephytox.fr/accueil). After harvesting, queen scallops were transported to the laboratory, washed and scrubbed of epibionts, and immediately subjected to conditioning for toxin depuration.

2.2. Experimental design and sampling

The *in vivo* DA-depuration experiment was performed as described by Vanmaldergem *et al.* (2023) with modifications. The animals were placed in a flow-through 100 L-tank supplied with filtered seawater (4 µm, activated carbon, flow rate of 70 $mL \cdot min^{-1}$, complete renewal in 24 h to avoid re-ingestion of feces) and daily fed with *Tisochrysis lutea* (clone *T.iso*) (Bendif *et al.*, 2013) at a concentration of 5×10^5 $cells \cdot scallop \cdot day^{-1}$. The inlet flow of running seawater was cut off for 4 h prior to each feeding to ensure microalgae ingestion. The water was maintained fully oxygenated (100 % O_2 saturated), at a temperature of 14 ± 1 °C, and the salinity of the pumped seawater within the Bay (*i.e.* ~34 PSU). The organisms were maintained under these experimental conditions for 30 days, with sequential sampling of 5 animals after 0, 5, 8, 12, 19, and 30 days of depuration in the laboratory.

Sampled scallops were placed on crushed ice to avoid suffering during sacrifice. The meat was excised from the shells, and since the digestive gland (DG) accumulates ≥ 80 % of total DA burdens in other pectinid species (*e.g., P. maximus*, Blanco *et al.*, 2002a, 2020) this organ was carefully dissected, and was the main target of this study. The DG of each animal was separated from the rest of the tissues to avoid contamination by DA during dissections (García-Corona *et al.*, 2022) and sliced into two halves, one stored at -20 °C to determine the toxin concentration in each individual, and the other half was fixed in Davidson solution (Kim *et al.*, 2006) for anti-DA immunohistochemical purposes. The rest of the tissues (RT = adductor muscle, gills, mantle, kidney, and gonad) were entirely stored in Davidson solution for DA-immunohistochemistry.

2.3. Domoic acid extraction and HPLC-UV analysis

Toxin was extracted exclusively from the DG of each scallop by homogenizing 200 ± 10 mg of frozen tissue in 1 mL of 50 % MeOH:H_2O (Quilliam *et al.*, 1989) using a Fastprep-24 5 G system (MP Biomedicals, Sta. Ana, CA, USA). Homogenates were clarified by

centrifugation at 19,000× *g* at 4 °C, filtered through 0.22 µm nylon syringe filters (VWR International, Radnor, PA, USA), and stored at -20 °C until analysis. Afterward, DA was quantified as described in García-Corona *et al.* (2022). The HPLC System was equipped with a UV spectrophotometer Waters 996 PDA-UV detector. The column used was a C_{18} Jupiter HPLC (Phenomenex 250 × 4.6 mm, 5 µm) with a gradient of the mobile phase ranging from 5% to 25% of CH_3CN and 0.1% of CF_3COOH. The injection volume was 20 µL and the run time was set at 20 min with a flow rate of 1mL min^{-1}. The column temperature was maintained at 40 °C. The detection wavelength was set at 242 nm. Certified DA standard was purchased from the National Research Council of Canada (NRC) and quantification was performed from a six-point calibration curve obtained by serial dilutions in MeOH: H_2O (1:1, *v/v*) with concentrations between 0.2 to 8 µg DA mL^{-1} (r = 0.99). The limits of detection (LODs) of the HPLC system ranged from 0.2 to 1 mg DA kg^{-1} tissue.

2.4. Histology and DA-immunohistochemistry

In order to expand knowledge about the anatomical localization of DA in different tissues of *A. opercularis*, a specific anti-DA immunohistochemical protocol recently developed by García-Corona *et al.* (2022) was applied in this work. Tissues embedded in paraffin were thin-sectioned (4-µm) in triplicate for each sample and used for (i) immunohistochemical detection of DA (IHC), (ii) multichromic staining, and (iii) hematoxylin/eosin staining (H&E), as described below. For IHC analyses, sections were deparaffinized, rehydrated, and incubated overnight with a dilution (0.01 mg·mL^{-1}) of a Goat polyclonal anti-DA primary antibody (Eurofins Abraxis®, Warminster, PA, USA) at 4 °C. The next day, the slides were incubated at 37 °C for 2 h with a dilution (0.001 mg·mL^{-1}) of an HRP-sharped IgG Rabbit anti-Goat secondary antibody (abcam®, Cambridge, UK). Finally, samples were revealed with diaminobenzidine (DAB+Chromogen Substrate Kit, abcam®, Cambridge, UK) for 1 h in darkness at room temperature. The second slide from each sample was stained with a multichromic procedure (Costa and Costa, 2012) consisting of a combination of Alcian Blue and Periodic Acid–Schiff's for the demonstration of acid mucopolysaccharides and neutral glycoconjugates, in blue and magenta tones, respectively, Hematoxylin blueing for nuclear materials, and picric acid to identify proteins in yellow

hues. The last set of tissue sections was stained with routinary histological staining Hematoxylin–Eosin as a reference (Kim *et al.,* 2006).

In García-Corona *et al.* (2024b) DA was localized within autophagosome-like vesicles (*i.e.* early DA-autophagy) but mainly in post-autophagic residual bodies (*i.e.* late DA-autophagy) in the cytoplasm of the digestive cells of *A. opercularis*. Therefore, to better understand the implications of autophagic mechanisms in the sequestration and toxicokinetics of DA in the DG of this species, five regions from each histological section of the DG from each scallop treated with the anti-DA IHC protocol (*i.e.,* 150 micrographs in total) were randomly digitized at high resolution (63 × magnification; 600 dpi). Then, total numbers of autophagome-like vesicles and residual bodies, as well as total numbers of autophasome-like vesicles and residual bodies with positive DA-chromogenic signal present in a predetermined area of ~1.33 mm^2 were counted as an estimation of the occurrence of total and DA-autophagy in the whole DG of the scallops through the entire depuration process (García-Corona *et al.,* 2024b).

2.5. Statistical analysis

All statistical analyses were performed using command lines in the R language (R v. 4.0.2, R Core Team, 2022) on the basic module Rstudio. *A priori* Lilliefors (Kolmogorov-Smirnov) and Fligner-Killeen tests, were applied to assess the normality of frequencies of the data, and the heterogeneity of variances, respectively (Hector, 2015). When needed, data were transformed (log, ln, $1/\chi$, or $\sqrt{\chi}$) before analysis to meet *a priori* assumptions, but all data are reported untransformed as the mean ± standard error (SE). Separate one-way analyses of variance (ANOVA, type II Sum of Squares) were used to determine statistically significant differences in toxin concentrations in the DG, as well as in the frequencies of total and anti-DA labeled autophagosome-like vesicles and residual bodies in the digestive glands of the scallops. The depuration rate of DA in the DG was calculated according to Dusek Jennings *et al.* (2020) using the one-compartment exponential decay model, $DAt = DA_0 \cdot e^{-rt}$, where DA*t* is the DA concentration after *t* days, DA_0 represents DA concentration at the end of the depuration, *t* is days elapsed, and the slope of the equation (*r*) is the daily depuration rate. DA_0 and the slope were estimated using linear regression after ln-

transformation of DA burdens (Álvarez *et al.*, 2020), but untransformed data are presented. Differences were considered statistically significant at $\alpha = 0.05$ for all analyses (Zar, 2010).

3. Results

3.1. Toxin depuration

The amounts of DA measured in the DG of the scallops decreased slightly from ~40 to ~30 $mg \cdot kg^{-1}$ within the first 12 days of conditioning in the laboratory, and to 17.3 ± 3.4 $mg \cdot kg^{-1}$ at the end of the experiment (*i.e.*, after 30 days). Nonetheless, these differences in DA burdens in the DG were not significant (Fig.1). The coefficients of variation (CV) ranged between 30 to 80 % throughout the entire depuration experiment, which reflected a significant inter-individual variability in DA concentration in the DG between individuals. As shown in Fig.1, DA depuration rate in the DG of the scallops was estimated at 0.018 day^{-1} from a one-compartment exponential decay model that explained 30 % of the variance, with a good statistical fit ($P < 0.05$) and without evidence of over-dispersion of the data. The straight-line relationship of ln-transformed DA concentrations indicates that depuration rate was slight but constant over the course of the experiment (Fig. 1).

3.2. Anatomical and subcellular localization of domoic acid

The brown chromogenic signal (cs) corresponding to DA was readily detected by IHC at the subcellular level in the DG of scallops over the entire 1-month decontamination period. As observed in Fig. 2A-2B, the anti-DA immune signal was observed mainly within bigger residual bodies (rb) of ~10 µm of diameter distributed in the basal region of the cytoplasm of digestive cells. Particularly, the anti-DA residual bodies were localized in the adipocyte-like cells (al) in the acinar region (ar) of the digestive diverticula (dd) in the DG. The multichromic and the H&E staining (Fig. 2C-D and 2E-F, respectively) showed that the small autophagosome-like vesicles (~ 1 µm diameter) gathered giving rise to residual bodies in the cytoplasm of the adipocyte-like digestive cells of the digestive diverticula. No specific histopathologies related to the accumulation of toxins were observed in the DG of the animals. Notwithstanding, an intense process of vacuolization (v) of the digestive cells of the scallops was found (Fig. 2C-F). As shown in Fig. 2E&F, neither the autophagosome-like vesicles nor the resulting residual bodies with positive DA immunoreactivity acquired any dye with the H&E staining. Moreover, no differences ($P > 0.05$) were found in the total

numbers of autophagosome-like vesicles and residual bodies, nor in the frequencies of anti-DA autophagosome like-vesicles and anti-DA residual bodies in the DG of the scallops throughout the entire depuration period (Table I).

The anatomical localization of the toxin in the rest of the tissues was the same in all analyzed scallops (Fig. 3). The DA-labeling was detected mainly in the microvilli that line the branchial filaments (Fig. 3A), in the axons of the neurons embedded between the bundles of the adductor muscle (Fig. 3B), and within the globose mucus-producing cells embedded in the spawning ducts in both male and female portions of the gonads (Fig. 3C and 3D, respectively). Finally, no brown anti-DA signal was observed in the mantle nor the kidney of the scallops.

4. Discussion

Farmers and fishermen in northern Europe ask for alternative resources to compensate for harvest closures of heavily DA-contaminated stocks of the slow depurator *P. maximus.* Nonetheless, to propose alternative resource is a complicated task with gaps in knowledge about the depuration kinetics of this toxin in other exploitable species such as the queen scallop *A. opercularis*. In this work, for the first time, the kinetics of DA-depuration were assessed in the DG of naturally contaminated queen scallops under controlled depuration conditions. Furthermore, the time-tracking of DA-localization was *in situ* measured at the subcellular level in the DG through depuration process by means of a specific anti-DA IHC technique recently developed by García-Corona *et al.* (2022) in order to unveil the physiological mechanisms behind DA-depuration kinetics in this species. Scallops toxicity during and after toxic *Pseudonitzschia*-blooms is determined on one hand by total amounts of DA and, on the other hand, by depuration of a part of DA initially accumulated mainly in the DG (Dusek Jennings *et al.*, 2020; García-Corona *et al.*, 2024a,b). Thus, understanding the biological mechanisms involved in DA-decontamination is of the utmost importance since the toxicity of shellfish beds, and the consequent exploitation capacity of these resources is determined mainly by the depuration kinetics.

Although a high inter-individual variability in DA contents was found in queen scallops in this study, these large variations in toxin burdens, particularly in the DG (CV ranging from 12 to 125 %) seem to be a characteristic of slow DA-depurator species, as reported for *P.*

maximus (Bogan *et al.*, 2007; García-Corona *et al.*, 2024a). Moreover, depuration rates of DA can also widely vary between bivalve species. Most fast DA-depurators like mussels and oysters (Silvert and Subba, 1992; Wohlgeschaffen *et al.* 1992; Novaczek *et al.*, 1992; Jones *et al.*, 1995; Mafra *et al.*, 2010; Bresnan *et al.*, 2017; Blanco *et al.* 2002b) and several clams (Gilgan *et al.* 1990; Álvarez *et al.*, 2015; Dusek Jennings *et al.*, 2020; Blanco *et al.*, 2010) are capable of depurate DA burdens over hours to days, while other species such as the clam *S. patula* require many months to depurate DA from their tissues (Horner and Postel, 1993; Trainer and Bill, 2004; Dusek Jennings *et al.*, 2020). Notwithstanding, pectinids seem to be a controversial group within bivalves in their way of depurating DA. Although species such as *A. purpuratus* (Álvarez *et al.*, 2020) and *P. magellanicus* (Wohlgeschaffen *et al.*, 1992; Douglas *et al.*, 1997) are considered as fast depurators (0.9 and 0.25 day^{-1} in the DG, respectively), others such as *P. maximus* exhibit the slowest depuration rates (0.008 to 0.001 day^{-1}) registered among shellfish species (Blanco *et al.*, 2006; García-Corona *et al.*, 2024a).

The depuration rate of DA in the DG of *A. opercularis* estimated in this work was about 0.02 day^{-1}, which is very similar to that calculated in the same organ of the slow depurator *S. patula* (Horner and Postel, 1993). It was thus assumed that, with a level of contamination as low as 40 mg DA kg^{-1} of DG, it would still take nearly 70 days (*i.e.*, more than two months) for the scallops of this experiment to depurate total DA burdens accumulated in the DG. This means that DA detoxification kinetics in *A. opercularis* is nearly 11 and 50-fold slower than those reported for the fast depurator scallops *P. magellanicus* (0.2 day^{-1}) and *A. purpuratus* (0.9 day^{-1}), respectively, and ~10-fold faster than the slowest DA depurator *P. maximus* (0.001 to 0.008 day^{-1}) in digestive tissues. It is important to highlight that this slow depuration kinetics and the repeated and intense seasonal blooms of toxic *Pseudo-nitzschia* could worsen the scenario leading to contaminated queen scallops for several months throughout the year, which may pose a serious threat to public health. Some strategies such as the evisceration of highly contaminated organs (*i.e.*, the DG) have been applied by the profession to discard heavily DA-contaminated non-edible organs (*e.g.*, the DG) and leave only less contaminated (< 20 mg kg^{-1}, according to sanitary threshold, Wekell *et al.*, 2004) edible tissues (*e.g.*, muscle and gonad) of the commercially important *P. maximus*. Whereas the only alternative to accelerate DA detoxification would be keeping

contaminated scallops at aquaculture facilities free of particulate and dissolved DA. Nevertheless, both options mentioned above are not economically feasible considering the cost of such procedures, and the space and food production required for the conditioning of scallops (F. Breton, pers com, 2023; Vanmaldergem *et al.,* 2023). Indeed, the total depuration time of *A. opercularis* in DA-free water systems would be 12 times greater than the six days suggested by Vanmaldergem *et al.* (2023) as economically affordable to maintain DA-contaminated scallop stocks under these detoxification conditions. Notwithstanding, it is also important to mention that during the same bloom of toxic *P. australis* of this work, it was reported that adult specimens of *P. maximus* were strongly contaminated with up to 638.6 ± 35.5 mg DA kg^{-1} in the DG (García-Corona *et al.*, 2024b), which is 17-fold more DA in the same organ than the queen scallops in this study. Although there is evidence that in adult king scallops there is no relationship between shell length and DA concentrations, it seems that smaller individuals have faster DA uptake and more efficient depuration capabilities (Bogan *et al.*, 2007). It thus appears that juvenile *A. opercularis* have much lower contamination and greater detoxification capacities than adult *P. maximus* when cohabiting the same areas affected by toxic *Pseudo-nitzschia* blooms of the same intensity. Therefore, considering adult queen scallops as a substitute resource for other slow-depurator pectinid species strongly contaminated during and after ASP outbreaks such as *P. maximus* is feasible but must be cautious, and its exploitation should take into account the DA-depuration rate of this species as well as the toxin concentrations in fishery stocks.

Despite the economic and ecological consequences associated with such long retention of DA in slow depurators, the mechanisms underlying this phenomenon in affected species are still not fully understood. It has been demonstrated that digestive cells have a particular contribution to the high accumulation and long retention time of DA in the DG of some bivalves through the activation of different molecular and subcellular mechanisms. Up to 90 % of total DA burdens are accumulated in a free and soluble form in the cytoplasm of the digestive cells (Blanco *et al.,* 2006; Lage *et al.,* 2012), and in some species like *P. maximus,* the long retention of this toxin has been hypothesized to be due to the lack of some efficient membrane transporter proteins to excrete DA out of the cells (Mauriz and Blanco *et al.*, 2010). Other mechanisms such as the presence of low-affinity glutamate

receptors in all tissues, and the selective activation of high DA capacity sites in specific tissues (*e.g.*, the siphon) are the only explanation so far for long DA-retention of this toxin in *S. patula* (Trainer and Bill, 2004).

At the subcellular level, our findings put in evidence that after DA-ingestion, and through the decontamination period, an intense process of late-autophagy was activated with the formation of DA-residual bodies in the digestive cells of *A. opercularis*. The intramuscular injection of DA in *P. maximus* activated the upregulation of genes related to autophagy in the DG of *P. maximus* (Ventoso *et al.,* 2021). Moreover, the accumulation of DA has proven to trigger *in situ* autophagic processes in the DG of different contaminated shellfish species, such as *C. fornicata* (García-Corona *et al.,* 2024b), but particularly in the scallops *P. maximus* and *A. opercularis* (García-Corona *et al.,* 2022; 2024a,b). Autophagy is a catabolic system that removes from the cell unnecessary, dysfunctional, or potentially harmful components employing a lysosome-dependent regulated mechanism (Balbi *et al.*, 2018; Picot *et al.*, 2019; Wang *et al.,* 2019; Zhao *et al.*, 2021). This highly conserved process allows the orderly degradation or recycling of cellular compounds playing a major role in the homeostasis of non-starved cells (Klionsky, 2008; Mizushima and Komatsu, 2011; Wang *et al.*, 2019). Through early autophagy, specific cytoplasmic components are targeted and isolated within small double-membrane bounded vesicles called autophagosomes (Xie and Klionsky, 2007; Yurchenko and Kalachev, 2019). Consequently, autophagosomes fuse with the lysosomes bringing its specialty process of waste management and disposal out of the cell (Mizushima *et al.*, 2011; Parzych and Klionsky, 2014; Zhao *et al.*, 2021). In some cases, when the enzymatic battery of the lysosomes is unable to degrade the cargo materials within the autophagosomes, these small vesicles aggregate giving rise to larger residual bodies (late autophagy) that remain for long time in the cytoplasm of the cell, blocking the excretion of undigested or indigestible materials (Mathers, 1976; Cuervo, 2004; McMillan and Harris, 2018; Yurchenko and Kalachev, 2019). Using immunostaining of DA, most of the toxin-labeling was found within a large number of residual bodies distributed in the adipocyte-like cells of the digestive diverticula of *A. opercularis* as recently reported by García-Corona *et al.* (2024b) for *C. fornicata* and *A. opercularis,* and for *P. maximus* through DA-depuration process (García-Corona *et al.*, 2024b). The anti-DA staining in this work revealed that in *A. opercularis* the amount of

toxin sequestered within autophagosomes during early autophagy is negligible, and most of DA is trapped in post-autophagic residual bodies that appeared immediately after the toxic bloom of *P. australis* and remained in the digestive diverticula with the same intensity and prevalence among the 30 days of depuration period, this despite the rapid 24-h cycles of digestive cell regeneration exhibited by pectinids (Owen, 1972; Mathers, 1976). Through the application of the same anti-DA immunohistochemical method, it was demonstrated that late autophagy, with the formation of residual bodies in digestive cells, is a mechanism strongly correlated with sequestration and long retention of a part of DA initially accumulated in *P. maximus* that took place ~30 days after toxic *P. australis* outbreaks, resembling a kind of analogous DA-tattoo that remains indefinitely in the DG of scallops (García-Corona *et al.*, 2024a). In king scallops, it was thus hypothesized that: 1) DA may undergo successive cycles of capture–release–recapture by autophagy through the regenerative cycle of digestive cells of the scallops, or 2) DA-laden residual bodies could exhibit long lifespans without any toxin vanishing from months to years (García-Corona *et al.*, 2024a). Although the subcellular time-tracking of late-autophagy in this work revealed no significant differences in the frequencies of anti-DA residual bodies across the depuration experiment, the temporal differences in the formation of these post-autophagic structures between *A. opercularis* (immediately after) and *P. maximus* (one month later) lead to hypothesize that part of DA accumulated in the DG of queen scallops remains trapped within these structures less time than in king scallops, but also suggest that *A. opercularis* process DA derived from toxic *Pseudo-nitzschia* faster than *P. maximus.* All these together strengthen the second hypothesis proposed by García-Corona *et al.* (2024a) on the long persistence of residual bodies bearing DA in the DG of contaminated scallops, and put in evidence that late-autophagy may be a part of the explanation for the slow DA depuration rate in *A. opercularis.*

The anatomical distribution of DA in the rest of the tissues of the queen scallop was very similar to that observed by García-Corona *et al.* (2022, 2024a) in *P. maximus*, since a well-localized anti-DA chromogenic signal was found in neuronal structures, but mainly in the mucus lining the microvilli of the branchial filaments, as well as in the mucus-producing globose cells embedded in the spawning ducts in the gonads. The chemical affinity DA-mucus in *P. maximus*, and now in *A. opercularis*, is still unclear. Whereas in fast depurators

such as *A. purpuratus* (Álvarez *et al.*, 2020), *Mesodesma donacium* (Álvarez *et al.*, 2015) as well as *M. edulis, M. galloprovincialis,* and *Crassostrea virginica* (Blanco *et al.*, 2002b; Mafra *et al.*, 2010), up to 90% of total DA burdens are rapidly transferred from the DG to other body compartments (*i.e.* the gonad, mantle, gills, muscle, and kidney) for independent and much more efficient excretion, in slow detoxifiers, like *P. maximus*, less than 5% of total DA accumulated in the DG is transferred to other organs for excretion (Blanco *et al.*, 2002a, 2006). Therefore, further analyses are needed to elucidate the role of mucus and the rest of the tissues in DA-depuration in *A. opercularis*.

This work represents a cornerstone in the untangling of DA-depuration kinetics in *A. opercularis*. Further transcriptomic and proteomic analyses are required to delve into physiological reasons for the slow DA-depuration in this species and to elucidate if there are other mechanisms besides late-autophagy, such as the absence of membrane transporters, or the presence of high-capacity receptors, blocking the excretion of DA out the cells in this and other affected shellfish species.

5. Conclusions

The depuration rate of DA in the digestive gland of *A. opercularis* assessed here revealed that this species can remain contaminated for a few months, hence, this species cannot be considered a fast DA-detoxifier. Furthermore, the subcellular time-tracking of this toxin in the DG of queen scallops suggests that the occurrence of long-persistent DA-labeled residual bodies through the depuration process is a physiological mechanism presumably involved in the strenuous removal of a portion of DA initially accumulated in the scallops. The results of this work constitute an important step forward in the knowledge about the physiological mechanisms involved in DA-toxicokinetics in this important species for fisheries and aquaculture on the eastern Atlantic coast and should be taken into account by the profession when making decisions about its exploitation after toxic *Pseudo-nitzschia* blooms. The evidence presented here could be of great value to feed numerical models that compare or predict the depuration in different species of affected invertebrates, as well as in the proposal of strategies to accelerate DA-depuration in queen scallops.

Conflict of interest

All authors approved the final version of this manuscript and declared no conflict of interest or misconduct behavior.

Funding

This work received financial support from the research project “MaSCoET” (Maintien du Stock de Coquillages en lien avec la problématique des Efflorescences Toxiques) financed by France Filière Pêche and Brest Métropole. JLGC was recipient of a doctorate fellowship from CONACyT, Mexico (REF: 2019-000025-01EXTF-00067).

Data availability statement

The evidence and data that support the findings of this study are available from the corresponding author upon reasonable request.

Ethics statements

The juvenile scallops (*Aequipecten opercularis*) used in this work were transported and handled according to the International Standards for the Care and Use of Laboratory Animals. The number of sampled animals contemplated the rule of maximizing information published and minimizing unnecessary studies. In this sense, 30 scallops were considered as the minimum number of organisms needed for this study.

Acknowledgments

The authors are infinitely grateful to Sylvain Enguehard (Novakits, Nantes) for providing the non-commercial anti-DA primary antibodies necessary to carry out this study, as well as Jacques Grall and Franck Quéré for help with scallop collection. We also thank Margot Deleglise (LEMAR, Brest) and Carmen Rodríguez-Jaramillo (CIBNOR, La Paz) for technical assistance with HPLC-UV analyses, and advices to optimize noncommercial antibodies for the IHC analysis, respectively.

References

Álvarez, G., Rengel, J., Araya, M., Álvarez, F., Pino, R., Uribe, E., Díaz, P.A., Rossignoli, A.E., López-Rivera, A., Blanco, J. 2020. Rapid Domoic Acid Depuration in the Scallop

462 *Argopecten purpuratus* and Its Transfer from the Digestive Gland to Other Organs.
463 *Toxins*, 12, 698. https://doi.org/10.3390/toxins12110698.
464 Álvarez, G., Uribe, E., Regueiro, J., Martin, H., Gajardo, T., Jara, L., Blanco, J. 2015.
465 Depuration and anatomical distribution of domoic acid in the surf clam *Mesodesma*
466 *donacium*. *Toxicon*, 102, 1–7. https://doi.org/10.1016/j.toxicon.2015.05.011.
467 Amzil, Z., Fresnel, J., Le Gal, D., Billard, C. 2001. Domoic acid accumulation in French
468 shellfish in relation to toxic species of *Pseudo-nitzschia multiseries* and *P.*
469 *pseudodelicatissima*. *Toxicon*, 39(8), 1245–1251. https://doi.org/10.1016/s0041-
470 0101(01)00096-4.
471 Balbi, T., Cortese, K., Ciacci, C., Bellese, G., Vezzulli, L., Pruzzo, C., Canesi, L. 2018.
472 Autophagic processes in *Mytilus galloprovincialis* hemocytes: effects of *Vibrio tapetis*.
473 *Fish & Shellfish Immunology*, 73, 66–74. https://doi.org/10.1016/j.fsi.2017.12.003.
474 Basti, L., Hegaret, H., Shumway, S.E. 2018. Harmful Algal Blooms and Shellfish. In
475 Shumway, S.E., Burkholder, J.M., Morton, S.L., eds. Harmful Algal Blooms a
476 Compendium Desk Reference, pp.135–191. John Wiley & Sons Inc., Hoboken, NJ.
477 Bates SS, Bird CJ, Freitas ASWd, Foxall R, Gilgan M, Hanic LA, Wright JLC. 1989.
478 Pennate diatom *Nitzschia pungens* as the primary source of domoic acid, a toxin in
479 shellfish from Eastern Prince Edward Island, Canada. *Canadian Journal of Fisheries*
480 *and Aquatic Sciences*, 46: 1203–1215.
481 Bates, S.S., Hubbard, K.A., Lundholm, N., Montresor, M., Leaw, C.P. 2018. *Pseudo-*
482 *nitzschia*, *Nitzschia*, and domoic acid: new research since 2011. *Harmful Algae*, 79, 3–
483 43. https://doi.org/10.1016/j.hal.2018.06.001.
484 Beukers-Stewart B.D., Beukers-Stewart J.S. 2009. Principles for the Management of
485 Inshore Scallop Fisheries around the United Kingdom. Report to Natural England,
486 Scottish Natural Heritage and Countryside Council for Wales. Marine Ecosystem
487 Management Report no. 1, University of York, 58 pp.
488 Blanco, J., Acosta, C. P., Mariño, C., Muñiz, S., Martín, H., Moroño, Á., Correa, J.,
489 Arévalo, F., Salgado, C. 2006. Depuration of domoic acid from different body
490 compartments of the king scallop *Pecten maximus* grown in raft culture and natural bed.
491 *Aquatic Living Resources*, 19(3), 257–265. http://dx.doi.org/10.1051/alr:2006026

492 Blanco, J., Acosta, C., Bermúdez de la Puente, M., Salgado, C. 2002a. Depuration and
493 anatomical distribution of the amnesic shellfish poisoning (ASP) toxin domoic acid in
494 the king scallop *Pecten maximus*. *Aquatic Toxicology*, 60 (1-2), 111–121.
495 https://doi.org/10.1016/s0166-445x(01)00274-0.
496 Blanco, J., Bermúdez, M., Arévalo, F., Salgado, C., Moroño, A. 2002b. Depuration of
497 mussels (*Mytilus galloprovincialis*) contaminated with domoic acid. *Aquatic Living*
498 *Resources*, 15, 53–60. https://doi.org/10.1016/S0990-7440(01)01139-1.
499 Blanco, J., Livramento, F., Rangel, I. M., 2010. Amnesic shellfish poisoning (ASP) toxins
500 in plankton and molluscs from Luanda Bay, Angola. *Toxicon*, 55(2–3), 541–546.
501 https://doi.org/10.1016/j.toxicon.2009.10.008.
502 Blanco, J., Mauríz, A., Álvarez, G. 2020. Distribution of Domoic Acid in the Digestive
503 Gland of the King Scallop *Pecten maximus*. *Toxins*, 12(371): 1-11.
504 http://dx.doi.org/10.3390/toxins12060371.
505 Bogan, Y. M., Harkin, A. L., Gillespie, J., Kennedy, D. J., Hess, P., Slater, J. W. 2007. The
506 influence of size on domoic acid concentration in king scallop, *Pecten maximus* (L.).
507 *Harmful Algae*, 6(1): 15–28. https://doi.org/10.1016/j.hal.2006.05.005.
508 Bresnan, E., Fryer, R. J., Fraser, S., Smith, N., Stobo, L., Brown, N., Turrell, E. 2017. The
509 relationship between *Pseudo-nitzschia* (Peragallo) and domoic acid in Scottish shellfish.
510 *Harmful Algae*, 63, 193–202. https://doi.org/10.1016/j.hal.2017.01.004.
511 Costa, P., Costa, M.H. 2012. Development and application of a novel histological
512 multichrome technique for clam histopathology. *Journal of Invertebrate Pathology*, 110,
513 411-414. http://dx.doi.org/10.1016/j.jip.2012.04.013.
514 Cuervo, A. M. 2004. Autophagy: Many paths to the same end. *Molecular and Cellular*
515 *Biochemistry*, 263(1/2), 55–72. https://doi.org/10.1023/b:mcbi.0000041848.57020.57.
516 Douglas, D.J., Kenchington, E.R., Bird, C.J., Pocklington, R., Bradford, B., Silvert, W.
517 1997. Accumulation of domoic acid by the sea scallop (*Placopecten magellanicus*) fed
518 cultured cells of toxic *Pseudo-nitzschia multiseries*. *Canadian Journal of Fisheries and*
519 *Aquatic Sciences*, 54 (4), 907–913. https://doi.org/10.1139/f96-333.
520 Dusek Jennings, E., Parker, M. S., Simenstad, C. A. 2020. Domoic acid depuration by
521 intertidal bivalves fed on toxin-producing *Pseudo-nitzschia multiseries*. *Toxicon*, 6,
522 100027. https://doi.org/10.1016/j.toxcx.2020.100027.

García-Corona, J. L., Fabioux, C., Vanmaldergem, J., Petek, S., Derrien, A., Terre-Terrillon, A., Bressolier, L., Breton, F., & Hegaret, H. 2024a. The amnesic shellfish poisoning toxin, domoic acid: The tattoo of the king scallop *Pecten maximus. Harmful Algae*, 133, 102607. https://doi.org/10.1016/j.hal.2024.102607.

García-Corona, J. L., Hégaret, H., Deléglise, M., Marzari, A., Rodríguez-Jaramillo, C., Foulon, V., Fabioux, C. 2022. First subcellular localization of the amnesic shellfish toxin, domoic acid, in bivalve tissues: Deciphering the physiological mechanisms involved in its long-retention in the king scallop *Pecten maximus*. *Harmful Algae*, 116. https://doi.org/10.1016/j.hal.2022.102251.

García-Corona, J.L., Hegaret, H., Lassudrie-Duchesne, M., Derrien, A., Terre-Terrillon, A., Delaire, T., Fabioux, C. 2024b. Comparative study of domoic acid accumulation, isomer content and associated digestive subcellular processes in five marine invertebrate species. *Aquatic Toxicology*, 266, 106793 https://doi.org/10.1016/j.

Gilgan, M.W. 1996. Fish Inspection Services, Department of Fisheries and Oceans, Canada. Unpublished data.

Gilgan, M.W., Burns B.G., Landry, G.J. 1990. Distribution and magnitude of domoic acid contamination of shellfish in Atlantic Canada. In: E. Graneli, B. Sundstrom, L. Edler, D.M. Anderson (Eds.), Toxic Marine Phytoplankton. Elsevier, N.Y. pp. 469- 474.

Hector, A., 2015. The new statistics with R: an introduction for biologists, 1st ed. Oxford University Press, New York.

Horner, R.A., Kusske, M.B., Moynihan, B.P., Skinner, R.N. Wekell, J.C. 1993. Retention of Domoic Acid by Pacific Razor Clams, *Siliqua patula* (Dixon, 1789): Preliminary Study. *Journal of Shellfish Research*, 12, 451-456.

Horner, R.A., Postel, J.R. 1993. Toxic diatoms in western Washington waters (U.S. west coast). Hydrobiologia, 269: 197–205. https://doi.org/10.1007/BF00028018.

Husson, B., Hernández-Fariñas, T., Le Gendre, R., Schapira, M., Chapelle, A. 2016. Two decades of *Pseudo-nitzschia spp*. blooms and king scallop (*Pecten maximus*) contamination by domoic acid along the French Atlantic and English Channel coasts: Seasonal dynamics, spatial heterogeneity and interannual variability. *Harmful Algae*, 51, 26–39. https://doi.org/10.1016/j.hal.2015.10.017.

553 Jones, T.O., Whyte, J.N.C., Ginther, N.G., Townsend, L.D., Iwama, G.K., 1995.
554 Haemocyte changes in the pacific oyster, *Crassostrea gigas*, caused by exposure to
555 domoic acid in the diatom *Pseudo-nitzschia pungens* f. multiseries. *Toxicon,* 33 (3),
556 347–353. https://doi.org/10.1016/0041-0101(94)00170-.
557 Kim, Y., Ashton-Alcox, K.A. Powell, E.N. 2006. Histological Techniques for Marine
558 Bivalve Molluscs: update. NOAA Technical Memorandum NOS NCCOS 27, Maryland.
559 Klionsky, D. J. 2008. Autophagy revisited: A conversation with Christian de Duve.
560 *Autophagy*, 4(6): 740–743. https://doi.org/10.4161/auto.6398.
561 La Barre, S., Bates, S.S., Quilliam, M.A. 2014. Domoic acid. In. Outstanding marine
562 molecules: chemistry, biology, analysis. Edited by S. La Barre and J.-M. Kornprobst.
563 Wiley-VCH Verlag GmbH & Co. KgaA, Weinheim, Germany, pp. 189–216.
564 Lage, S., Raimundo, J., Brotas, V., Costa, P.R., 2012. Detection and sub-cellular
565 distribution of the amnesic shellfish toxin, domoic acid, in the digestive gland of
566 *Octopus vulgaris* during periods of toxin absence. *Marine Biology Research,* 8, 784–
567 789. https://doi.org/10.1080/17451000.2012.659668.
568 Leal, J. F., & Cristiano, M. L. S. 2024. Why are bivalves not detoxified? *Current Opinion*
569 *in Food Science,* 57, 101162. https://doi.org/10.1016/j.cofs.2024.101162.
570 Lefebvre, K. A., Robertson, A. 2010. Domoic acid and human exposure risks: A review.
571 *Toxicon*, 56(2), 218–230. http://dx.doi.org/10.1016/j.toxicon.2009.05
572 Lelong, A., H´egaret, H., Soudant, P., Bates, S.S. 2012. *Pseudo-nitzschia*
573 (Bacillariophyceae) species, domoic acid and amnesic shellfish poisoning: revisiting
574 previous paradigms. *Phycologia,* 51 (2), 168–216. https://doi.org/10.2216/11-37.1.
575 Mafra Jr., L.L., Bricelj, V.M., Fennel, K. 2010. Domoic acid uptake and elimination
576 kinetics in oysters and mussels in relation to body size and anatomical distribution of
577 toxin. *Aquatic Toxicology*, 100, 17–29. https://doi.org/10.1016/j.aquatox.2010.07.0.
578 Mathers, N.F. 1976. The effects of tidal currents on the rhythm of feeding and digestion in
579 *Pecten maximus* L. *Journal of Experimental Marine Biology and Ecology*, 24 (3), 271–
580 283. https://doi.org/10.1016/0022-0981(76)90059-9.
581 Mauriz, A., Blanco, J. 2010. Distribution and linkage of domoic acid (amnesic shellfish
582 poisoning toxins) in subcellular fractions of the digestive gland of the scallop *Pecten*
583 *maximus*. *Toxicon,* 55(2-3), 606–611. https://doi.org/10.1016/j.toxicon.2009.10.

McKenzie JD, Bavington C. 2002. Measurement of Domoic Acid in King Scallops processed in Scotland. Final Report for The Food Standards Agency Scotland. https://www.foodstandards.gov.scot/downloads/Domoic_Acid_in_King_Scallops.pdf

McMillan, D.B., Harris, R.J., 2018. The Animal Cell. In: An Atlas of Comparative Vertebrate Histology (pp. 3–25). Elsevier. https://doi.org/10.1016/b978-0-12-410424-2.00001-9.

Miller, M.A., Moriarty, M.E., Duignan, P.J., Zabka, T.S., Dodd, E., Batac, F.I., Young, C., Reed, A., Harris, M.D., Greenwald, K., Kudela, R.M., Murray, M.J., Gulland, F.M.D., Miller, P.E., Hayashi, K., Gunther-Harrington, C.T., Tinker, M.T., Toy-Choutka, S. 2021. Clinical Signs and Pathology Associated With Domoic Acid Toxicosis in Southern Sea Otters (*Enhydra lutris nereis*). *Frontiers in Marine Science*, 8. https://doi.org/10.3389/fmars.2021.585501

Mizushima, N., Komatsu, M. 2011. Autophagy: Renovation of Cells and Tissues. *Cell*, 147(4): 728–741. https://doi.org/10.1016/j.cell.2011.10.026.

Novaczek, I., Madhyastha, M. S., Ablett, R. F., Donald, A., Johnson, G., Nijjar, M. S., Sims, D. E. 1992. Depuration of Domoic Acid from Live Blue Mussels (*Mytilus edulis*). *Canadian Journal of Fisheries and Aquatic Sciences*, 49(2), 312–318. https://doi.org/10.1139/f92-035.

Owen, G., 1972. Lysosomes, peroxisomes and bivalves. *Science Progress*, 60 (239), 299–318.

Parzych, K.R., Klionsky, D.J. 2014. An Overview of Autophagy: Morphology, Mechanism, and Regulation. Antioxidants & Redox Signaling, 20(3): 460–473. https://doi.org/10.1089/ars.2013.5371.

Perl, T.M., Bedard, L., Kosatsky, T., Hockin, J.C., Todd, E.C., Remis, R.S. 1990. An out-break of toxic encephalopathy caused by eating mussels contaminated with domoic acid. *The New England Journal of Medicine*, 322, 1775–1780. https://doi.org/10.1056/NEJM199006213222504.

Picot, S., Morga, B., Faury, N., Chollet, B., Dégremont, L., Travers, M.A., Renault, T., Arzul, I., 2019. A study of autophagy in hemocytes of the Pacific oyster *Crassostrea gigas*. *Autophagy*, 1–9. https://doi.org/10.1080/15548627.2019.1596.

Pulido, O.M. 2008. Domoic Acid Toxicologic Pathology: A Review. *Marine Drugs*, 6, 180-219. https://doi.org/10.3390/md20080010.

Quilliam, M. A., Sim, P. G., McCulloch, A. W., McInnes, A. G. 1989. High-Performance Liquid Chromatography of Domoic Acid, a Marine Neurotoxin, with Application to Shellfish and Plankton. *International Journal of Environmental Analytical Chemistry*, 36(3), 139–154. https://doi.org/10.1080/03067318908026867.

Ramsdell, J.S. 2007. The molecular and integrative basis to domoic acid toxicity. In: Botana L (ed), Phycotoxins: Chemistry and Biochemistry, Blackwell Publishing Professional, Cambridge, MA, USA, 223–50.

Silvert, W., Subba R.D.V. 1992. Dynamic model of the flux of domoic acid, a neurotoxin, through a *Mytilus edulis* population. *Canadian Journal of Fisheries and Aquatic Sciences*, 49, 400- 405. https://doi.org/10.1139/f92-045.

Trainer, V. L., Bates, S. S., Lundholm, N., Thessen, A. E., Cochlan, W. P., Adams, N. G., Trick, C. G. 2012. *Pseudo-nitzschia* physiological ecology, phylogeny, toxicity, monitoring and impacts on ecosystem health. *Harmful Algae*, 14, 271–300. http://dx.doi.org/doi:10.1016/j.hal.2011.10.025

Trainer, V.L. Bill, B.D. 2004. Characterization of a domoic acid binding site from Pacific razor clam. *Aquatic Toxicology*, 69, 125–132. http://dx.doi.org/10.1016/j.aquatox.2004.04.012.

Vanmaldergem, J., García-Corona, J.L., Deléglise, M., Fabioux, C., Hegaret, H. 2023. Effect of the antioxidant N-acetylcysteine on the depuration of the amnesic shellfish poisoning toxin, domoic acid, in the digestive gland of the king scallop *Pecten maximus*. *Aquatic Living Recourses*, 36, 14. https://doi.org/10.1051/alr/2023011.

Ventoso, P., Pazos, A.J., Blanco, J., Pérez-Parallé, M.L., Triviño, J.C., Sánchez, J.L. 2021. Transcriptional Response in the Digestive Gland of the King Scallop (*Pecten maximus*) after the Injection of Domoic Acid. *Toxins*, 13, 339. https://doi.org/10.3390/toxins13050339.

Wang, L., Ye, X., Zhao, T. 2019. The physiological roles of autophagy in the mammalian life cycle. *Biological Reviews*, 94, 503–516. https://doi.org/10.1111/brv.12464.

Wekell, J.C., Hurst, J., Lefebvre, K.A. 2004. The origin of the regulatory limits for PSP and ASP toxins in shellfish. *Journal of Shellfish Research*, 23: 927–930.

Wohlgeschaffen, G. D., Mann, K. H., Subba Rao, D. V., Pocklington, R. 1992. Dynamics of the phycotoxin domoic acid: accumulation and excretion in two commercially important bivalves. *Journal of Applied Phycology*, 4(4), 297–310. https://doi.org/10.1007/bf02185786.

Xie, Z., Klionsky, D. J. 2007. Autophagosome formation: core machinery and adaptations. *Nature Cell Biology*, 9(10): 1102–1109. https://doi.org/10.1038/ncb1007-1102.

Yurchenko, O., Kalachev, A. 2019. Morphology of nutrient storage cells in the gonadal area of the Pacific oyster, *Crassostrea gigas* (Thunberg, 1793). *Tissue Cell*, 56, 7–13. https://doi.org/10.1016/j.tice.2018.11.004.

Zabaglo, K., Chrapusta, E., Bober, B., Kaminski, A., Adamski, M., Bialczyk, J. 2016. Environmental roles and biological activity of domoic acid: A review. *Algal Research*, 13, 94–101. http://dx.doi.org/10.1016/j.algal.2015.11.020.

Zar, J. H., 2010. Biostatistical Analysis. 5th Ed. Pearson, Westlake Village, CA, 251 pp.

Zhao, Y. G., Codogno, P., Zhang, H. 2021. Machinery, regulation and pathophysiological implications of autophagosome maturation. *Nature Reviews Molecular Cell Biology*. http://dx.doi.org/10.1038/s41580-021-00392-4.

Table I. Total numbers of autophagosome-like vesicles (Ta) and residual bodies (Trb), as well as anti-DA labeled autophagosome-like vesicles (DAa) and residual bodies (DArb) in the digestive glands of scallops *A. opercularis* across the depuration process in the laboratory for 30 days after a natural DA-contamination event during toxic *Pseudo-nitzschia spp.* outbreak on the northwest coast of France in early April 2021.

	Time (days elapsed)						Statistical analysis	
	0	5	8	12	19	30		
Ta	11 ± 2.2^{a}	9.2 ± 1.6^{a}	10.2 ± 3.2^{a}	9 ± 1.6^{a}	8.2 ± 1.2^{a}	9.8 ± 2.4^{a}	$F_{(df = 5,24)} = 0.9$;	$P > 0.05$
Trb	8.2 ± 1.6^{a}	8.6 ± 1.5^{a}	8.8 ± 1.2^{a}	13.8 ± 3.7^{a}	10 ± 2.4^{a}	10 ± 1.3^{a}	$F_{(df = 5,24)} = 0.5$;	$P > 0.05$
DAa	6.6 ± 1.9^{a}	4 ± 1.6^{a}	4.4 ± 1.9^{a}	3.2 ± 1.2^{a}	3.6 ± 1.1^{a}	4 ± 1.4^{a}	$F_{(df = 5,24)} = 0.6$;	$P > 0.05$
DArb	7 ± 1.8^{a}	6.8 ± 1.6^{a}	6 ± 0.7^{a}	10 ± 2.1^{a}	6.8 ± 1.9^{a}	5.2 ± 0.8^{a}	$F_{(df = 5,24)} = 0.4$;	$P > 0.05$

Results are expressed as mean (autophagosomic structures. area^{-1}) ± SE. Data were analyzed using the sampling time (six levels) as independent variable in separate one-way ANOVA's. The *F*-test statistic and degrees of freedom (*df*) are reported. Different superscript letters denote statistically significant differences between groups. The level of statistical significance was set at $\alpha = 0.05$.

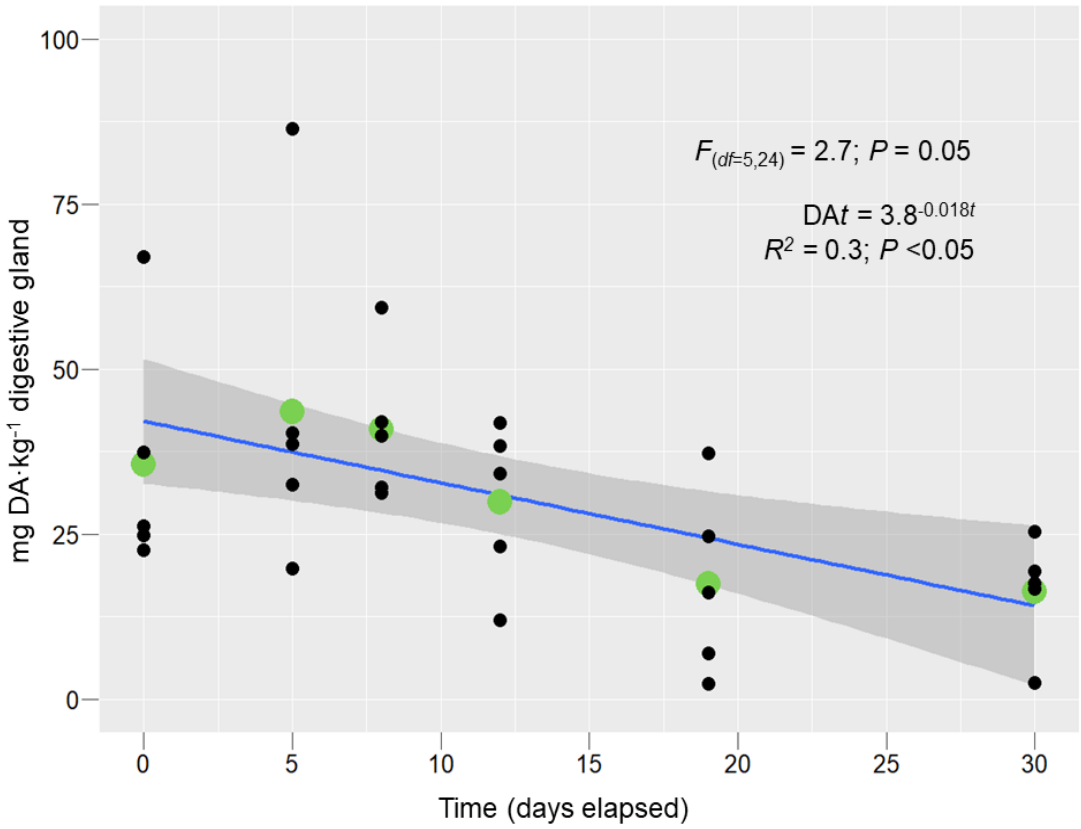

Figure 1. Concentrations of DA in the digestive glands of scallops *A. opercularis* across the depuration process in the laboratory for 30 days after a natural DA-contamination event during toxic *Pseudo-nitzschia* spp. outbreak on the northwest coast of France in early April 2021. The black dots are the individual observations, and the larger green dots are the means. The daily DA depuration rate was calculated using the one-compartment exponential decay model, $DAt = DA_0 \cdot e^{-rt}$, where DA*t* is the DA concentration after *t* days, DA_0 represents DA concentration at the end of the depuration, *t* is days elapsed, and the slope of the equation (*r*) is the daily depuration rate. DA_0 and the slope were estimated using linear regression (blue line, R^2 ± standard deviation) after ln-transformation of DA burdens, but untransformed data are presented. Data on DA concentrations were analyzed using the sampling time (six levels) as independent variable in a one-way ANOVA. The *F*-test statistic and degrees of freedom (*df*) are reported. The level of statistical significance was set at $\alpha = 0.05$.

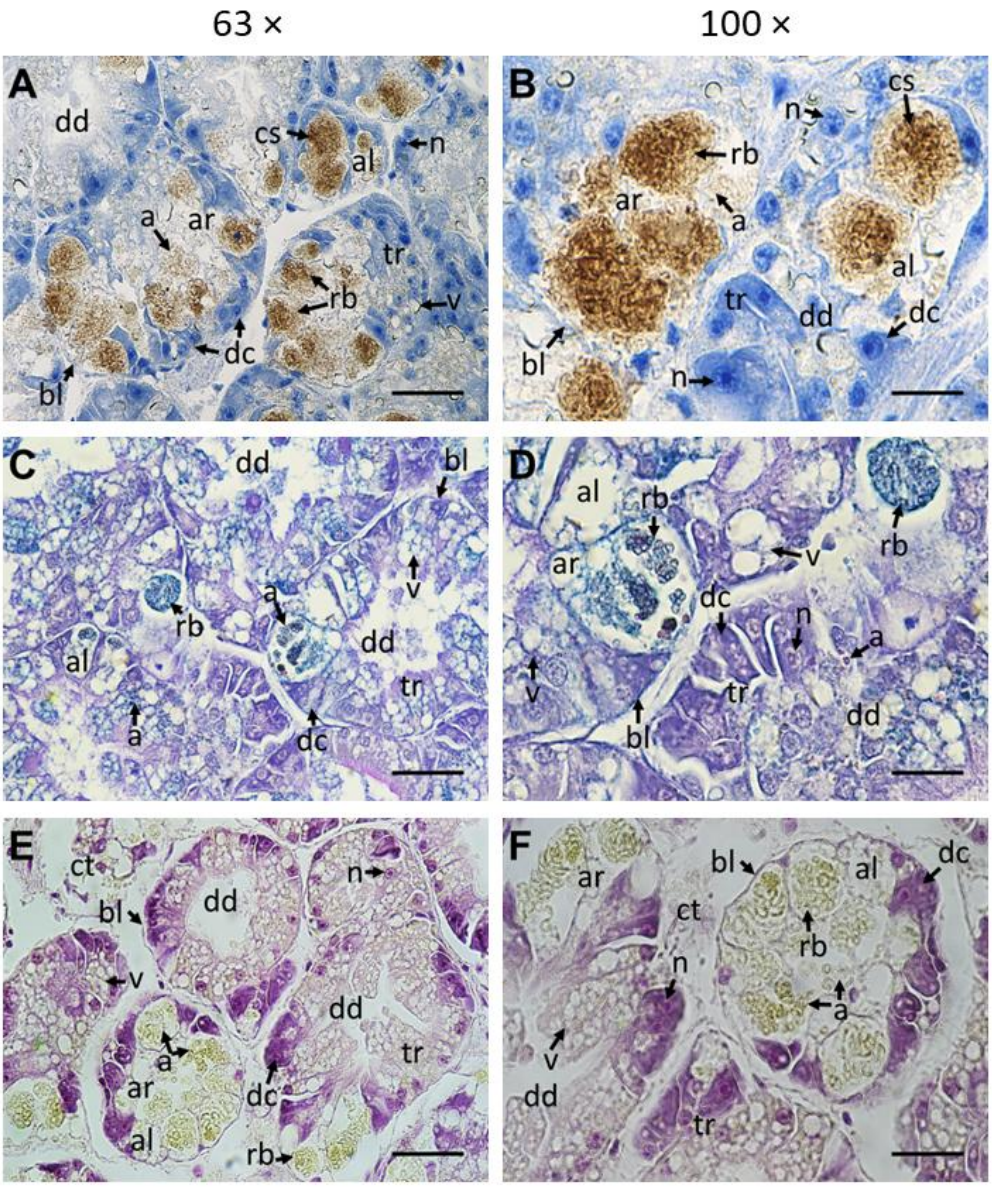

683

684 **Figure 2.** Microphotographs of digestive glands of naturally DA-contaminated scallops *A.*
685 *opercularis* collected after outbreaks of toxic *Pseudo-nitzschia* spp. in the northwest coast
686 of France in early April 2021 and representative of the entire DA-depuration process in the
687 laboratory through 30 days. (A, B) = Immunohistochemical detection of DA using specific
688 anti-DA antibody (0.08 mg. mL^{-1}); (C, D) = multichromic histochemical staining of neutral
689 carbohydrates (violet-magenta dyes), acid glycoconjugates (blue hues), and proteins
690 (yellowish tones); (E, F) = conventional histological Hematoxylin-Eosin staining. a =
691 autophagosomic-like vesicles, al = adipocyte-like cell, ar = acinar region, bl = basal lamina,
692 cs = DA chromogenic signal, ct = connective tissue, dc = digestive cells, dd = digestive
693 diverticulum, n = nucleus, rb = residual bodies, tr = tubular region, v = vacuoles. Scale bar:
694 63 × = 30 µm, 100 × = 10 µm.

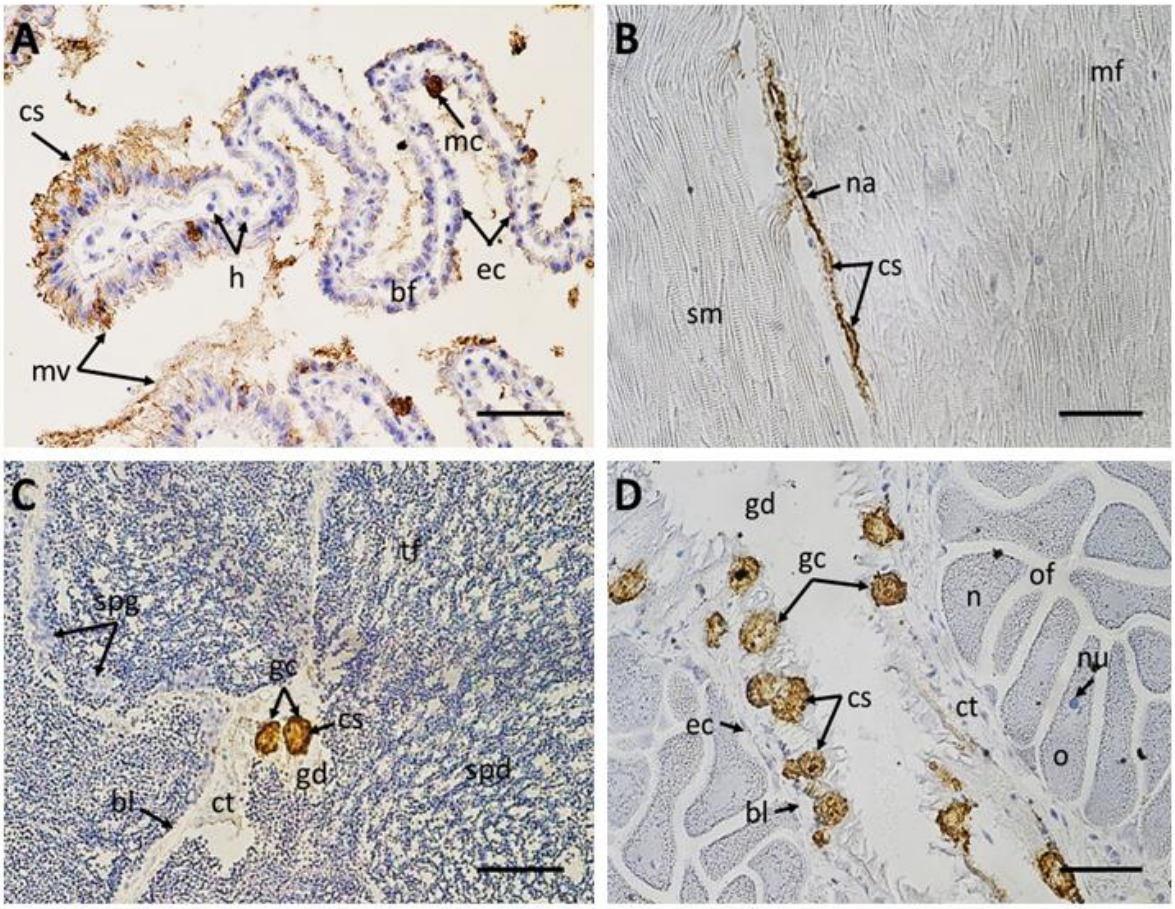

Figure 3. Microphotographs of the rest of tissues (A, gills; B, adductor muscle; C, male gonad; D, female gonad) of naturally DA-contaminated scallops *A. opercularis* collected after outbreaks of toxic *Pseudo-nitzschia* spp. in the northwest coast of France in early April 2021 and representative of the entire DA-depuration process in the laboratory through 30 days. Specific anti-DA immunohistochemical (IHC) staining appeared in brown hues on the images. bf = branchial filament, bl = basal lamina, cs = positive anti-DA chromogenic signal, ct = connective tissue, ec = epithelial cell, gc = globose cell, gd = gonadal duct, h = hemocytes, mv = microvilli, n = nucleus, na = neuronal axon, nu = nucleolus, o = oocyte, of = ovarian follicle, sm = striated muscle, spd = spermatids, spg = spermatogonia, tf = testicular follicle. Scale bar: 40× = 50 µm.